USING AN ENCOMPASSING PERIODIC BOX TO PERFORM NUMERICAL CALCULATIONS ON GENERAL DOMAINS

PATRICK GUIDOTTI

ABSTRACT. This paper shows how numerical methods on a regular grid in a box can be used to generate numerical schemes for problems in general smooth domains contained in the box with no need for a domain specific discretization. The focus is mainly be on spectral discretizations due to their ability to accurately resolve the interaction of finite order distributions (generalized functions) and smooth functions. Mimicking the analytical structure of the relevant (pseudo-differential) operators leads to viable and accurate numerical representations and algorithms. An important byproduct of the structural insights gained in the process is the introduction of smooth kernels (at the discrete level) to replace classical singular kernels which are typically used in the (numerical) representations of the solution. The new kernel representations yield enhanced numerical resolution and, while they necessarily lead to significantly higher condition numbers, they also suggest natural and effective ways to precondition the systems.

1. INTRODUCTION

It is the primary goal of this paper to develop a framework which allows one to extend the benefits of numerical spectral methods from boxes to arbitrary geometry domains. The idea is to simulate problems on domains $\Omega \subset B$ located inside a periodicity box $B = [-\pi, \pi]^n$ by using spectral approximation of generalized functions (distributions). This is best illustrated in the case of boundary value problems, which are also an important application of the method. Consider the boundary value problem

$$\begin{cases} \mathcal{A}u = f & \text{in } \Omega, \\ \mathcal{B}u = g & \text{on } \partial\Omega, \end{cases}$$

for some generic differential operator $\mathcal{A}$ and boundary operator $\mathcal{B}$. It is no restriction to assume that the operators and the data be defined everywhere in the box B. One obtains a numerical approximation for the boundary value problem in the following manner. First discretize the periodicity box B by a regular grid $G^m = \{x_j^m : j \in \mathbb{Z}_n^m\}$ with 2^{mn} points if working in dimension $n \in \mathbb{N}$, then, independently, discretize the boundary Γ of the domain Ω by a subset $\Gamma^n = \{y_1, \ldots, y_n\} \subset \Gamma$. Choose a discretization A^m of the operator $\mathcal{A}$ which operates on the grid G^m and find a solution $v^m : G^m \to \mathbb{R}$ of

$$A^m v^m = f^m$$

in G^m for a discretization of f. With that in hand, generate numerical approximations for functions $\psi_k^m : G^m \to \mathbb{R}$, $k = 1, \ldots, n$, in the kernel of the operator $\mathcal{A}_\Omega$ on Ω and try to adjust the solution v^m by a linear combination

$$w^{m,n} = \sum_{k=1}^n w_k^{m,n} \psi_k^m$$

of these kernel elements in order for $u^{m,n} = v^m + w^{m,n}$ to satisfy a discretization $\mathcal{B}^{m,n} u^{m,n} = g^n$ of the boundary condition for a discretization $g^n : \Gamma^n \to \mathbb{R}$ of g. Choosing $\mathcal{B}$ to be the trace operator

---

Key words and phrases. Spectral methods, meshless methods, numerical analysis, boundary value problems.

γ_Γ at first for ease of presentation, this can be done as follows. Approximate δ_{y_k} for $k = 1, \dots, n$ by its spectral representation $\delta_{y_k}^m$ on the periodic grid G^m and insist that

$$\langle \delta_{y_j}^m, u^{m,n} \rangle_{q^m} = g_j^n, \; j = 1, \dots, n,$$

where $\langle \cdot, \cdot \rangle_{q^m}$ is the discrete duality pairing (scalar product) discretizing the continuous duality pairing $\langle \cdot, \cdot \rangle_{\mathcal{D}_\pi', \mathcal{D}_\pi}$ between periodic distributions and testfunctions. Details will be given in the rest of the paper. Following the strategy outlined above leads to a system for the unknown $w^{m,n}$ of the form

$$\langle \delta_{y_j}^m, w^{m,n} \rangle_{q^m} = \sum_{k=1}^n \langle \delta_{y_k}^m, \psi_k^m \rangle_{q^m} w_k^{m,n} = \sum_{k=1}^n M_{jk} w_k^{m,n} = g_j^n - \langle \delta_{y_j}^m, v^m \rangle_{q^m}, \; j = 1, \dots, n,$$

One can think of $\delta_{y_.}^m$ as the discrete kernel of the trace operator γ_Γ. It is therefore possible to deal with a more general boundary operator $\mathcal{B}$ by deriving a "natural" numerical approximation $B_{y_j}^m$ of its distributional kernel for $j = 1, \dots, n$. This would lead to the system

$$\langle B_{y_j}^m, w^{m,n} \rangle_{q^m} = \sum_{k=1}^n \langle B_{y_j}^m, \psi_k^m \rangle_{q^m} w_k^{m,n} = g_j^n - \langle B_{y_j}^m, v^m \rangle_{q^m}, \; j = 1, \dots, n,$$

In order to obtain a numerical method it remains to generate the kernel functions ψ_k^m for $k = 1, \dots, m$. This can be done in many different ways. In order to, at first, make a connection explicit to pseudo-differential operators, again consider $\mathcal{B} = \gamma_\Gamma$ and procede in the following manner. Take the spectral approximation $\delta_{y_k}^m$ for $k = 1, \dots, n$ and set

$$\psi_k^m = (A^m)^{-1} \delta_{y_k}^m.$$

Since the Dirac distribution is "supported" on the singleton $\{y_k\}$, the function ψ_k^m will indeed "lie" in the kernel of A^m over Ω. Since these functions are "peaked" at different locations y_k, they will be linearly independent. The matrix M in the system for the unknown $w^{m,n}$ is therefore given by

$$M_{jk} = \langle \delta_{y_j}^m, (A^m)^{-1} \delta_{y_k}^m \rangle_{q^m}, \; j, k = 1, \dots, n.$$

Latter can be recognized as the discrete counterpart of

$$m(y, \eta) = \langle \delta_y, \mathcal{A}^{-1} \delta_\eta \rangle, \; y, \eta \in \Gamma,$$

the distributional kernel of a pseudodifferential operator on the boundary curve Γ. This connection is made more precise in the rest of the paper and provides a framework in which to obtain analytical proofs for the numerical methods introduced. For implementation purposes, however, it is best to proceed in a somewhat different way when constructing the kernel functions ψ_k^m. Instead of using the "rougher" Dirac distributions used above, it is better to replace them by smooth functions $\varphi_{\tilde{y}_k}$ which are supported outside of Ω with support "centered" at $\tilde{y}_k = y_k + \delta \nu_\Gamma(y_k)$ for $\delta > 0$ where $\nu_\Gamma(y_k)$ is the unit outer normal to the boundary Γ at the point y_k. After discretization this leads to the alternative matrix

$$\widetilde{M}_{jk} = \langle \delta_{y_j}^m, (A^m)^{-1} \varphi_{\tilde{y}_k}^m \rangle_{q^m}, \; j, k = 1, \dots, n,$$

which is the discretization of a smoothing operator with kernel

$$\widetilde{m}(y, \eta) = \langle \delta_y, \mathcal{A}^{-1} \varphi_{\tilde{\eta}} \rangle, \; y, \eta \in \Gamma.$$

As such, M will be easier to capture numerically (fast convergent expansion of its kernel function) but also badly conditioned (as a smoothing and thus compact operator with unbounded inverse). In spite of this, "natural" and effective preconditioning procedures can be devised which completely remove this drawback. The rest of the paper is organized as follows. In the next section some preliminary results are obtained which highlight the main features of the underlying spectral approach to approximating generalized functions and testfunctions in the context of periodicity

and for boundary value problems, in particular; in Section 3 details are given about the discretizations used in the concrete examples studied in Section 4. The following section is dedicated to the specifics of the numerical implementation and to numerical experiments which illustrate the main theoretical insights and the advantages of the proposed method. A brief conclusion ends the paper.

2. Preliminaries

2.1. **Setup.** Before working with the relevant discretizations, the stage is set by fixing the analytical context which will very much guide the numerical procedures developed in the rest of the paper. Let $B = [-\pi, \pi)^n$ be the periodicity box bounding the area of interest. Extensive use will be made of distributions and of testfunctions. Latter are periodic smooth functions belonging to one of the following useful spaces

$$\mathcal{D}_\pi(B) = \mathcal{D}_\pi = \left\{ \varphi \in C^\infty(\mathbb{R}^n) \,\middle|\, \varphi \text{ is } 2\pi\text{-periodic} \right\} \tag{2.1}$$

$$\mathcal{D}_\pi^m(B) = \mathcal{D}_\pi^m = \left\{ \varphi \in C^m(\mathbb{R}^n) \,\middle|\, \varphi \text{ is } 2\pi\text{-periodic} \right\} \tag{2.2}$$

$$\mathcal{D}_0(B) = \mathcal{D}_0 = \left\{ \varphi \in C^\infty(\mathbb{R}^n) \,\middle|\, \text{supp}(\varphi) \subset\subset B \right\} \tag{2.3}$$

where $m \in \mathbb{N}$. The first space carries its standard locally convex topology generated by the family of seminorms $\{p_m : m \in \mathbb{N}\}$ given by

$$p_m(\varphi) = \sup_{|\alpha| \leq m} \|\partial^\alpha \varphi\|_\infty,$$

the second is a Banach with respect to the norm p_m, and the last carries the natural inductive limit-Fréchet topology, i.e. the coarsest topology which makes the inclusions

$$\mathcal{D}_K(B) = \left\{ \varphi \in C^\infty(\mathbb{R}^n) \,\middle|\, \text{supp}(\varphi) \subset K \right\} \hookrightarrow \mathcal{D}_0(B)$$

continuous for all $K = \overline{K} \subset\subset B$. Notice that $\mathcal{D}_K(B)$ is endowed with the locally convex topology induced by the seminorms

$$p_{m,K}(\cdot) = \sup_{|\alpha| \leq m} \|\partial^\alpha \cdot \|_{\infty,K},$$

where the additional subscript indicates that the supremum norm is taken over the set K. The space

$$\mathcal{D}_\pi'(B) = \mathcal{D}_\pi' = \left\{ u : \mathcal{D}_\pi \to \mathbb{K} \,\middle|\, u \text{ is linear and continous} \right\}$$

is then the space of $\mathbb{K}(= \mathbb{R}, \mathbb{C})$-valued distributions dual to $\mathcal{D}_\pi$. On $L_\pi^2 = L_\pi^2(B) = L^2(B)$ there is a natural orthonormal basis $(e_k)_{k \in \mathbb{N}}$ given by

$$e_k(x) = \frac{1}{(2\pi)^{n/2}} e^{ik \cdot x}, \ x \in B, \ k \in \mathbb{Z}^n,$$

consisting of eigenfunctions of the periodic Laplacian $-\Delta_\pi$. It is well-known that

$$\mathcal{F} : L_\pi^2 \to l^2(\mathbb{Z}^n), \ \varphi = \sum_{k \in \mathbb{Z}^n} \hat{\varphi}_k e_k \mapsto (\hat{\varphi}_k)_{k \in \mathbb{N}}$$

is an isometric isomorphism where

$$\hat{\varphi}_k = \int_B \varphi(x) \bar{e}_k(x) \, dx = \langle \varphi, \bar{e}_k \rangle = (\varphi | e_k).$$

In particular one has that $\|\varphi\|_{L_\pi^2} = \|(\hat{\varphi}_k)_{k \in \mathbb{N}}\|_{l^2(\mathbb{Z}^n)}$ and Parseval's identity

$$(\varphi | \psi) = \int_B \varphi \, \bar{\psi} \, dx = \sum_{k \in \mathbb{Z}^n} \hat{\varphi}_k \overline{\hat{\psi}_k} = (\hat{\varphi} | \hat{\psi}) \text{ for } \varphi, \psi \in L_\pi^2.$$

Notice that the formulæ above use the notations $\langle \cdot, \cdot \rangle$ and $(\cdot | \cdot)$ for the duality pairing and the scalar product, respectively. The former is clearly motivated by the natural duality pairing between distributions and test functions

$$\langle \cdot, \cdot \rangle : \mathcal{D}'_\pi \times \mathcal{D}_\pi \to \mathbb{K}, \ (u, \varphi) \mapsto \langle u, \varphi \rangle = u(\varphi).$$

Observe that, if $\varphi \in \mathcal{D}_\pi$, then $\partial^\alpha \varphi \in L^2_\pi$ for all $\alpha \in \mathbb{N}^n$ and thus

$$\partial^\alpha \sum_{k \in \mathbb{Z}^n} \hat{\varphi}_k e_k = \partial^\alpha \varphi = \sum_{k \in \mathbb{Z}^n} \widehat{(\partial^\alpha \varphi)}_k e_k = \sum_{k \in \mathbb{Z}^n} (ik)^\alpha \hat{\varphi}_k e_k,$$

with convergence in L^2_π, owing to well-known properties of the Fourier transform. Introducing the periodic Bessel potential spaces via

$$H^s_\pi = H^s_\pi(B) = \Big\{ u \in \mathcal{D}'_\pi \, \big| \, \sum_{k \in \mathbb{Z}^n} (1 + |k|^2)^s \hat{u}_k^2 < \infty \Big\},$$

for $s \in \mathbb{R}$ and $\hat{u}_k = \langle u, \bar{e}_k \rangle = (u | e_k)$, it follows easily that

$$\sum_{|k| \leq N} \hat{\varphi}_k e_k \to \varphi \text{ as } N \to \infty,$$

in H^s_π for any $s \geq 0$ if $\varphi \in \mathcal{D}_\pi$. By the well-known embedding

$$H^s_\pi \hookrightarrow C^m_\pi = C^m_\pi(B), \tag{2.4}$$

valid for $s > n/2 + m$, it then follows that the convergence of the Fourier series actually takes place in the topology of $\mathcal{D}_\pi$. An important consequence of this fact is the validity of the following generalized Parseval's identity

$$\langle u, \varphi \rangle = \langle u, \sum_{k \in \mathbb{Z}^n} \hat{\varphi}_k e_k \rangle = \sum_{k \in \mathbb{Z}^n} \underbrace{\langle u, e_k \rangle}_{=: \tilde{u}_k} \hat{\varphi}_k = \sum_{k \in \mathbb{Z}^n} \tilde{u}_k \hat{\varphi}_k, \tag{2.5}$$

$$(u | \varphi) = (u | \sum_{k \in \mathbb{Z}^n} \hat{\varphi}_k e_k) = \sum_{k \in \mathbb{Z}^n} (u | e_k) \hat{\varphi}_k = (\hat{u} | \hat{\varphi}) \tag{2.6}$$

for $u \in \mathcal{D}'_\pi$, $\varphi \in \mathcal{D}_\pi$, and $(u | e_k) = \langle u, \bar{e}_k \rangle = \langle u, e_{-k} \rangle$. A distribution $u \in \mathcal{D}'_\pi$ is said to be of finite order $m \in \mathbb{N}$ if it admits an estimate of the form

$$|\langle u, \varphi \rangle| \leq c \, p_m(\varphi), \ \varphi \in \mathcal{D}^m_\pi,$$

for a non-negative constant c but not for m replaced by $m - 1$. It follows from a density argument combined with the embedding (2.4) that any finite order distribution belongs to H^{-s}_π for some finite $s \geq 0$. The upshot of this is that (2.5) can be used to evaluate the action of a finite order distribution on a testfunction by a fast converging series since $(\tilde{u}_k)_{k \in \mathbb{N}}$ is polynomially bounded and $(\varphi_k)_{k \in \mathbb{N}}$ decays faster than the reciprocal of any polynomial in k. This combined with the choice of appropriate discretizations will be exploited later to derive highly accurate representations of various operators (not even necessarily supported on the discretization grid itself). Indeed many useful basic operations such as differentiation, integration, evaluation/interpolation are distributions of finite order. It also turns out that, for many interesting distributions $u \in \mathcal{D}'_\pi$, it will be possible to compute their Fourier coefficients either exactly or in a highly accurate manner.

2.2. **Simple Illustrative Examples.** Consider first δ_{x_0} for $x_0 \in B$ which is a zero order distribution. Later δ_{x_0} will be discretized on a regular grid but x_0 will be allowed to be any point in the domain B. Then it holds that

$$\delta_{x_0} = \sum_{k \in \mathbb{Z}^n} \langle \delta_{x_0}, e_k \rangle \bar{e}_k = \sum_{k \in \mathbb{Z}^n} (u | e_k) e_k.$$

Indeed

$$\langle \delta_{x_0}, \varphi \rangle = \langle \delta_{x_0}, \sum_{k \in \mathbb{Z}^n} \hat{\varphi}_k \rangle = \sum_{k \in \mathbb{Z}^n} \langle \delta_{x_0}, e_k \rangle \langle \varphi, \bar{e}_k \rangle = \langle \sum_{k \in \mathbb{Z}^n} (\tilde{\delta}_{x_0})_k \bar{e}_k, \varphi \rangle,$$

where $(\tilde{\delta}_{x_0})_k = e_k(x_0)$. The convergence of this evaluation series

$$\langle \delta_{x_0}, \varphi \rangle = \sum_{k \in \mathbb{Z}^n} e_k(x_0) \hat{\varphi}_k,$$

is clearly very fast and its coefficients are known either exactly or to a high degree of accuracy. This seemingly very simple observation will play a crucial role in the derivation of a highly accurate representation of higher dimensional kernels related to boundary value problems.

Remark 2.1. *While in this paper it will be enough to deal with the evaluation of smooth functions, such as test functions, in* [1] *modifications are presented (in a non-periodic context) which make it possible to retain good convergence properties also for piecewise smooth functions, another important class of functions in applications.*

The next example shows how the considerations of Subsection 2.1 provide an abstract framework in which to understand spectral methods (after discretization). Let $\varphi \in \mathcal{D}_\pi$ and consider computing

$$\partial^\alpha \varphi(x_0) = \langle (-1)^{|\alpha|} \partial^\alpha \delta_{x_0}, \varphi \rangle$$

at a point $x_0 \in B$. In this case

$$\partial^\alpha \varphi(x_0) = \langle (-1)^{|\alpha|} \partial^\alpha \delta_{x_0}, \varphi \rangle = \sum_{k \in \mathbb{Z}^n} (-1)^{|\alpha|} (\widetilde{\partial^\alpha \delta_{x_0}})_k \hat{\varphi}_k$$

$$= \sum_{k \in \mathbb{Z}^n} \partial^\alpha e_k(x_0) \hat{\varphi}_k = \sum_{k \in \mathbb{Z}^n} [(ik)^\alpha \hat{\varphi}_k] e_k(x_0).$$

It is again clear that the main advantages lie in the fact that φ is smooth and that the Fourier coefficients of $\partial^\alpha \delta_{x_0}$ are known exactly.

The next is an example of integration. Take $x_0 < x_1$ in the one dimensional box B. Of interest is the computation (eventually numerically) the integral

$$I(\varphi) = \int_{x_0}^{x_1} \varphi(x) \, dx$$

between the end points given (which are not necessarily on a numerical grid). Since $I \in \mathcal{D}'_\pi$ is a zero order distribution, it is possible compute its Fourier coefficients

$$\tilde{I}_k = \langle I, e_k \rangle = \int_{x_0}^{x_1} e_k(x) \, dx = \frac{1}{(2\pi)^{1/2}} \frac{1}{ik} [e^{ikx_1} - e^{ikx_0}],$$

again obtaining an explicit formula. Then

$$\int_{x_0}^{x_1} \varphi(x) \, dx = \sum_{k \in \mathbb{Z}} \tilde{I}_k \hat{\varphi}_k,$$

will provide a fast converging series representation.

2.3. **A simple Boundary Value Problem.** This section concludes with a simple example that will make the advantages and basic principle of this approach apparent. They will reappear in the higher dimensional context with the appropriate adjustments. Consider the following two point boundary value problem

$$\begin{cases} -\partial_{xx} u = f & \text{on } (x_0, x_1) \subset B, \\ u(x_j) = u_j & \text{for } j = 0, 1. \end{cases} \tag{2.7}$$

Notice that it will be considered as a problem embedded in the periodicity box B (which will later be discretized by a regular grid). Assume that $f \in \mathcal{D}_\pi$ be given along with $u_j \in \mathbb{R}$ for $j = 0, 1$. Choose a function $\psi \in \mathcal{D}_\pi$ satisfying

$$\hat{\psi}_0 = 1, \ 1 - \psi \in \mathcal{D}_0(B), \ \mathrm{supp}(\psi) \subset [x_0, x_1]^{\mathsf{c}},$$

and define

$$P_\psi f = f - \hat{f}_0 \psi$$

for the datum f and accordingly for any distribution in $\mathcal{D}_\pi'$. This way, a function $P_\psi f$ is obtained with vanishing average which coincides with f on (x_0, x_1). When applied to a general distribution u that is compactly supported inside the box, this operation produces a modified distribution $P_\psi u$ which coincides with the original u on its $\mathrm{supp}(u)$ if, without loss of generality, it is assumed that $\mathrm{supp}(u) \cap \mathrm{supp}(\psi) = \emptyset$. Next define the operator G_π acting on f via

$$\widehat{G_\pi(f)}_k = \begin{cases} 0, & k = 0, \\ \frac{\hat{f}_k}{k^2}, & k \neq 0 \end{cases}$$

so that

$$-\partial_{xx} G_\pi(f) = G_\pi(-\partial_{xx} f) = f - P_0(f),$$

for $P_0 f = f - \hat{f}_0 e_0$ is the orthogonal projection onto average free functions. A solution of (2.7) can be looked for in the form

$$u = G_\pi(P_\psi f) + v,$$

where v satisfies

$$\partial_{xx} v = 0 \text{ and } v(x_j) = u_j - G_\pi(P_\psi f)(x_j), \ j = 0, 1.$$

All that remains is to find two linearly independent elements v_0, v_1 in the kernel of $-\partial_{xx}$ on (x_0, x_1) and look for v in the form $v = \alpha_0 v_0 + \alpha_1 v_1$. In order for the boundary conditions to be satisfied, one needs that

$$\alpha_0 v_0(x_j) + \alpha_1 v_1(x_j) = u_j - G_\pi(P_\psi f)(x_j) =: \beta_j, \ j = 0, 1.$$

By choosing $v_k = G_\pi(P_\psi \delta_{x_k})$ for $k = 0, 1$, this leads to the matrix $M = [v_k(x_j)]_{j,k=0,1}$ with

$$M_{jk} = \langle \delta_{x_j}, G_\pi(P_\psi \delta_{x_k}) \rangle, \tag{2.8}$$

which is a kind of Green's function "$M = M(x_j, x_k)$", $j, k = 0, 1$. The crucial observation is that all ingredients $\delta_{x_j}, G_\pi, P_\psi \delta_{x_k}$ allow for spectral representations in the periodicity interval B (regardless of whether x_j for $j = 0, 1$ are or are not grid points after discretization). The convergence is, however, limited by the fact that, in (2.8), δ_{x_j} is of zero order and that $G_\pi(\tilde{\delta}_{x_k})$ is of limited smoothness (slightly better than H_π^1). This, however, can be alleviated by replacing $P_\psi \delta_{x_k}$ by either $P_\psi \delta_{\tilde{x}_k}$ with

$$\tilde{x}_k = x_k + \delta \nu(x_k) \text{ for } \nu(x_k) = (-1)^{k+1} \text{ and } k = 0, 1,$$

or, even better, by $P_\psi \varphi_{\tilde{x}_k}$ for a smooth test function $\varphi_{\tilde{x}_k} \in \mathcal{D}_0$ supported in a neighborhood U_k of $\tilde{x}_k$ with $U_k \cap (x_0, x_1) = \emptyset$ and $U_k \cap \mathrm{supp}(\psi) = \emptyset$ to obtain

$$\widetilde{M}_{jk} = \langle \delta_{x_j}, G_\pi(\tilde{\varphi}_{\tilde{x}_k}) \rangle.$$

It is easily checked that M is invertible for $x_0 \neq x_1$. Taking $\tilde{x}_k$ not too far from x_k and $\varphi_{\tilde{x}_k} \simeq \delta_{\tilde{x}_k}$, it follows that $\widetilde{M} \simeq M$ is also invertible. The upshot is, clearly, that $\widetilde{M}$ allows for a fast converging representation of its entries. To conclude this simple example one has that

$$u = G_\pi(P_\psi f) + [v_0 \ v_1] \widetilde{M}^{-1} \beta,$$

for $\beta = [\beta_0 \ \beta_1]^\top$.

Remark 2.2. *It is to be observed that, after discretization, all basic ingredients* $\delta_{x_j}, G_\pi, P_\psi \varphi_{\tilde{x}_k}, \psi$ *will have highly accurate grid representations, even if* $x_j, \tilde{x}_k$ *do not lie on the grid. Owing either to the availability of exact Fourier coefficients or to their smoothness, the additional discretization error incurred when going to a finite dimensional representation is as small as can be hoped for.*

3. Discretization

3.1. **One Dimension.** In order to rip the benefits of the above considerations the interval $B_1 = [-\pi, \pi)$ is discretized at $m \in \mathbb{N}$ (even) equidistant points $(x_j^m)_{j=0,\ldots,m-1}$ where

$$x_j^m = -\pi + \frac{2\pi}{m}j, \ j = 0, \ldots, m-1.$$

This will be sometimes referred to as the grid G_1^m of size m in dimension $n = 1$. As pointed out in [1], the choice of grid has to be complemented by an appropriate choice of corresponding quadrature rule $q^m = (q_j^m)_{j=0,\ldots,m-1}$ such that

$$\langle \mathbf{1}^m, \varphi^m \rangle_{q^m} = \mathbf{1}^m \cdot_{q^m} \varphi^m = q^m \cdot \varphi^m = \sum_{j=0}^{m-1} \varphi_j^m q_j^m \to \int_{B_1} \varphi(x)\, dx \text{ as } m \to \infty, \ \varphi \in \mathcal{D}_\pi,$$

for the constant function $\mathbf{1}$ with value 1 and for

$$\varphi^m = P_{\mathcal{P}}(\varphi) = \big(\varphi(x_j^m)\big)_{j=0,\ldots,m-1},$$

the (physical space) projection of the test function φ on the grid. It is also required that the quadrature rule satisfy

$$e_j^m \cdot_{q^m} \bar{e}_k^m = \delta_{jk}, \ 0 \leq j, k \leq m,$$

for the basis vectors e_j, $j = -m/2, \ldots, m/2 - 1$, where again the superscript indicates projection (by evalutation) on the grid.

Definition 3.1. *A discretization pair* (x^m, q^m) *on* B_1 *satsfying the above properties is called faithful discretization.*

The trapezoidal rule, for which it holds that

$$q^m = \frac{2\pi}{m}(1, \ldots, 1),$$

has this property of preserving the duality pairing and the orthogonal structure of the continuous setting. Many basic, useful distributions, such as δ_{x_0} for any $x_0 \in [-\pi, \pi)$, cannot be directly evaluated at points (short of obtaining a vanishing projection for all non-grid points x_0). It is then better to use an approximation based on Fourier coefficients and given by

$$u^m = P_{\mathcal{F}}(u) = \sum_{k=-m/2}^{m/2-1} \tilde{u}_k \bar{e}_k^m = \sum_{k=-m/2}^{m/1-2} \tilde{u}_k P_{\mathcal{P}}(\bar{e}_k), \ u \in \mathcal{D}_\pi.$$

The reason for this is that, in practice, one often has analytical knowledge of the coefficients $\tilde{u}_k$ or the ability to compute them to a high degree of accuracy.

Remark 3.2. *Observing that* $\delta_{x_0}^m = \sum_{k=-m/2}^{m/2-1} e_k(x_0)\bar{e}_k^m$ *and assuming that* $x_0 = x_{j_0}^m$ *is one of the grid points, one has that*

$$\delta_{x_{j_0}^m}^m(x_j^m) = \sum_{k=-m/2}^{m/2-1} e_k(x_{j_0}^m)\bar{e}_k(x_j^m) = \sum_{k=-m/2}^{m/2-1} e^{i(j_0-k)\pi} e_{j_0}(x_k^m)\bar{e}_j(x_k^m)e^{i(k-j)\pi}$$

$$= e^{i(j_0-j)\pi} \sum_{k=-m/2}^{m/2-1} e_{j_0}(x_k^m)\bar{e}_j(x_k^m) = e^{i(j_0-j)\pi} e_{j_0}^m \cdot_{q^m} \bar{e}_j^m$$

$$= \frac{m}{2\pi}\delta_{jj_0}$$

since

$$e_k(x_j^m) = \frac{1}{\sqrt{2\pi}}e^{-ik\pi+ik\frac{2\pi}{m}j} = \frac{1}{\sqrt{2\pi}}e^{i(j-k)\pi}e^{ij(-\pi+\frac{2\pi}{m}k)} = e^{i(j-k)\pi}e_j(x_k^m).$$

It is seen that $P_{\mathcal{F}}(\delta_{x_0})$ *evaluates exactly (to the discrete Dirac function) if* x_0 *is a grid point, while, for* $x_0 \in [-\pi,\pi) \setminus G_1^m$, *it has oscillatory character. In any case one has that*

$$\langle \delta_{x_0}^m, \varphi^m \rangle_{q^m} \to \langle \delta_{x_0}, \varphi \rangle = \varphi(x_0) \ as \ m \to \infty,$$

for any $\varphi \in \mathcal{D}_\pi$, *with fast convergence.*

Remark 3.3. *The alternating point trapezoidal rule of quadrature given by* $q^m = (2,0,\dots,2,0)$ *can also be used instead of the regular trapezoidal rule as it has been observed to have the required properties in* [1].

Definition 3.4. *The discrete Fourier transform* $\mathcal{F}_m : \mathbb{C}^m \to \mathbb{C}^m$ *is defined by*

$$\mathcal{F}_m(v) = \left(v \cdot_{q^m} \bar{e}_k^m\right)_{k=-m/2,\dots,m/2-1}, \ v \in \mathbb{C}^m.$$

Remark 3.5. *As the discretization is faithful,* $\mathcal{F}_m$ *is an isometric isomorphism. In fact it is easy to prove that*

$$v \cdot_{q^m} \overline{w} = \mathcal{F}_m(v) \cdot \overline{\mathcal{F}_m(w)}$$

so that Parseval's identity carries over exactly to the discrete setting. Notice that the standard Euclidean inner product is used in the right-hand side.

Proposition 3.6. *For a finite order distribution* $u \in \mathcal{D}_\pi'$ *and a test function* $\varphi \in \mathcal{D}_\pi$, *it can be shown (see* [1, Theorem 4.2] *and the considerations preceding it) that, given any* $N \in \mathbb{N}$, *one has that*

$$|\langle u, \varphi \rangle - u^m \cdot_{q^m} \varphi^m| \le c(P, u, \varphi)\frac{1}{m^N}.$$

Notice that, while this result is proved in [1] only for compactly supported distribution and compactly supported test functions, the same arguments apply in the current context since the compact support condition is not needed in the periodic context where no boundary is present and, hence, no boundary effects (read convergence slowdown due to boundary mismatch) can occur.

Remark 3.7. *At the continuous level, one can think of the series*

$$i(x,y) = \frac{1}{2\pi}\sum_{k\in\mathbb{Z}} e^{ik(x-y)}, \ x,y \in [-\pi,\pi),$$

as the (generalized, since it converges in the sense of distributions only) kernel i *of the identity map on* L_π^2 *since clearly*

$$\varphi(x) = \frac{1}{2\pi}\sum_{k\in\mathbb{Z}} e^{ikx}\int_0^{2\pi} e^{-iky}\varphi(y)\,dy \ \text{``}=\text{''} \int_0^{2\pi} i(x,y)\varphi(y)\,dy, \ \varphi \in \mathcal{D}_\pi.$$

In this context, a discretization which respects the duality pairing and the orthogonality structure as decribed above yields "natural" spectral discretizations for a variety of important operators which will be exploited later. In particular, it delivers such a discretization i^m for the identity map given by

$$(\delta_x^m|\delta_y^m) = \langle \delta_x^m, \bar{\delta}_y^m \rangle_{q^m} = \sum_{k,\tilde{k}=-m/2}^{m/2-1} e_k(x)\bar{e}_{\tilde{k}}(y)\langle \bar{e}_k^m, e_{\tilde{k}}^m \rangle_{q^m}$$

$$= \sum_{k,\tilde{k}=-m/2}^{m/2-1} e_k(x)\bar{e}_{\tilde{k}}(y)\delta_{k\tilde{k}} = \frac{1}{2\pi}\sum_{k=-m/2}^{m/2-1} e^{ik(x-y)} = i^m(x,y), \quad (3.9)$$

which is clearly the truncation of the series representation of the kernel i itself. Notice that x, y need not be grid points and that the approximation is thus "grid blind" and the error incurred is caused only by truncation of the series and by evaluation of the exponential function at the points of interest. If the kernel is evaluated on the grid points only, then it coincides with the kernel of discrete identity map, i.e. with the identity matrix

$$i^m(x_j^m, x_k^m) = \delta_{jk}.$$

3.2. **Higher dimensions.** In higher dimensions, the periodicity box $B = B_n$ is discretized analogously in each direction by equidistant points to obtain the grid

$$G^m = G_n^m = \underbrace{G_1^m \times G_1^m}_{n\text{-times}},$$

with corresponding quadrature rule $q^m = \left(\frac{2\pi}{m}\right)^n \mathbf{1}^m$, where now, $\mathbf{1}^m$ is thought of as a vector of length m^n. This way, a faithful discretization respecting duality pairing and orthogonality is obtained. In particular, it follows that

$$\langle e_k^m, \bar{e}_{\tilde{k}}^m \rangle_{q^m} = \delta_{k\tilde{k}},$$

for $e_k(x) = \frac{1}{(2\pi)^{n/2}} e^{ik \cdot x}$ for $x \in \mathbb{R}^n$, $k \in \mathbb{Z}^n$ and, again, $e_k^m = e_k\big|_{G^m}$. Dirac delta functions are approximated by tensor products

$$\delta_{x_0}^m = \delta_{x_0^1}^m \otimes \delta_{x_0^n}^m,$$

of the corresponding one dimensional representations $\delta_{x_0^j}^m$, $j = 1, \ldots, n$ where $x_0 = (x_0^j)_{j=1,\ldots,n}$. As far as test functions φ_{x_0} supported in a neighborhood of a point $x_0 \in B$ go, many choices can be made. The specifics will be given in the numerical experiments performed later. For now it is only important to know that such test functions can be given explicitly by an analytical formula which allows for accurate evaluation anywhere.

Consider now a general pseudodifferential operator $a(x, D)$ with symbol $\big(a(x,k)\big)_{k \in \mathbb{Z}^n}$ defined by

$$a(x,D)\varphi = \sum_{k \in \mathbb{Z}^n} e^{ik \cdot x} a(x,k)\hat{\varphi}_k,$$

and where $a(\cdot, k) : B \to \mathbb{C}$ is assumed to be smooth and periodic for each $k \in \mathbb{Z}^n$. Its Schwartz kernel is given by

$$k_a(x,y) = \sum_{k \in \mathbb{Z}^n} e^{ik \cdot (x-y)} a(x,k),$$

for which one has that

$$a(x,D)\varphi = \langle k_a(x,\cdot), \varphi \rangle \text{ for } \varphi \in \mathcal{D}_\pi.$$

More suggestively one can write that

$$k_a(x,y) = (\delta_x|a(x,D)\delta_y),$$

justified by the validity of the formal Parseval's identity

$$(\delta_x | a(x, D)\delta_y) = (\hat{\delta}_x | a\widehat{(x, D)}\delta_y) = \sum_{k \in \mathbb{Z}^n} e^{ik \cdot (x-y)} a(x, k).$$

If $a(x, \cdot)$ is polynomially bounded (for each x), convergence in the sense of distributions can be established. For well-known classes of symbols [2], it can be shown that k_a is smooth away from the diagonal $[x = y]$, where cancellations are responsible for the faster convergence of the series. This is the case for general differential operators and the corresponding solutions operators appearing in common boundary value problems, for instance. It turns out that, what was observed above for $a \equiv 1$ (leading to the identity map) in one space dimension, is valid for general pseudodifferential operators.

Theorem 3.8. *Given a pseudodifferential operator $a(x, D)$ with kernel k_a, it is natural to approximate it by the truncated series expansion*

$$k_a^m(x, y) = \sum_{k \in \mathbb{Z}_m^n} a(x, k) e^{ik \cdot (x-y)},$$

where $\mathbb{Z}_m^n = \left\{ k \in \mathbb{Z}^n : k_i = -m/2, \ldots, m/2 - 1 \text{ for } i = 1, \ldots, n \right\}$. In this case one has that

$$k_a^m(x, y) = (\delta_x^m | a^m(x, D)\delta_y^m), \tag{3.10}$$

for $a^m(x, D) = \mathcal{F}_m^{-1} a^m(x, \cdot) \mathcal{F}_m$ and

$$a^m(x, k) = a(x, k), \ k \in \mathbb{Z}_m^n.$$

Proof. In one dimension, the extension of (3.9) to general symbols amounts to

$$(\delta_x^m | a^m(x, D)\delta_y^m) = \left(\mathcal{F}_m(\delta_x^m) \big| \mathcal{F}_m[a^m(x, D)\delta_y^m] \right) = \sum_{k \in \mathbb{Z}_m^n} e^{ik \cdot x} a(x, k) e^{-ik \cdot y} = k_a^m(x, y),$$

since the term $\delta_{k\tilde{k}}$ in (3.9) is simply replaced by $a(x, \tilde{k})\delta_{k\tilde{k}}$. The rest follows from this and the fact that, in higher dimensions, one has that

$$\delta_x^m = \delta_{x_1}^m \otimes \cdots \otimes \delta_{x_n}^m \text{ and}$$

$$e_k(z) = e_{k_1}(z_1) \otimes \cdots \otimes e_{k_n}(z_n), \ z \in \mathbb{R}^n.$$

While only real valued symbols are considered here (because of the applications of interest), standard modification would allow to include the compex case as well. $\square$

This simple observation is quite useful and shows how to produce grid independent "spectral" approximations of operators through an approximation of their kernels. The structure of the kernel made apparent in (3.10) provides a blue print as to how to obtain numerical approximations to kernels of discrete operators K^m by simply computing $(\delta_x^m | K^m \delta_y^m)$. This is of interest when K^m is, for instance, the numerical inverse of the discretization A^m of an operator A for which no analytical inverse is available.

Remark 3.9. *For solution operators, the convergence of the series can, in general, be quite slow even if it is stronger than in the sense of distributions. This is due to the (mildly) singular behavior of the kernel on the diagonal and typically requires special care in the numerical evaluation process. Representation (3.10), however, suggests natural ways in which to do this by regularization of the kernel through*

$$\left(\delta_x^m | a^m(x, D)\varphi_{\tilde{y}}^m \right),$$

where $\mathcal{D}_\pi \ni \varphi_{\tilde{y}} \simeq \delta_{\tilde{y}}$ and $\tilde{y} \simeq y$ is conveniently located. In some cases, this modification can be carried out to obtain an alternate exact representation by a smooth kernel with no approximation involved. See the boundary value problem example in the next section.

4. Two Dimensional Examples

Two examples in two space dimensions are presented here which illustrate the benefits of the proposed approach.

4.1. **Integration.** Consider a (smooth or piecewise smooth) domain $\Omega \subset B$ and the numerical task of approximating the integral

$$I(\varphi) = \int_\Omega \varphi(x)\, dx, \ \varphi \in \mathcal{D}_\pi,$$

of a smooth function φ. Since I is a finite order distribution, one has that

$$I = \sum_{k \in \mathbb{Z}^2} \langle I, e_k \rangle \bar{e}_k = \sum_{k \in \mathbb{Z}^2} \tilde{I}_k \bar{e}_k,$$

and $I(\varphi) = \sum_{k \in \mathbb{Z}^2} \tilde{I}_k \hat{\varphi}_k$. If $\tilde{I}_k$ can be computed /approximated accurately by $\tilde{I}_k^m$ on G^m, then a numerical quadrature I^m for integration over Ω could be obtained by setting

$$I^m(\varphi^m) = \sum_{k \in \mathbb{Z}_m^2} \tilde{I}_k^m \hat{\varphi}_k^m,$$

where $\hat{\varphi}_k^m = \langle \varphi^m, \bar{e}_k^m \rangle_{q^m} = \mathcal{F}_m(\varphi)_k$ can be computed using the Fast Fourier transform. The notation $\mathbb{Z}_m^2$ is used, as before, for the appropriate set of indeces corresponding to the discretization level considered. While it appears that the problem of computing $I(\varphi)$ has simply been replaced by that of evaluating $I(e_k)$ for $k \in \mathbb{Z}_m^2$, the analytical knowledge of the bases functions and of their properties becomes useful. Indeed for $k = (0,0)$ one has

$$\tilde{I}_0 = \frac{1}{2\pi} \int_\Omega dx = \frac{1}{4\pi} \int_\Omega \mathrm{div}\begin{pmatrix} x_1 \\ x_2 \end{pmatrix} dx = \frac{1}{4\pi} \int_\Gamma (x_1 \nu_1 + x_2 \nu_2)\, d\sigma_\Gamma(x)$$

$$= \frac{1}{4\pi} \int_0^{2\pi} \left[\gamma_1(t)\dot{\gamma}_2(t) - \dot{\gamma}_1(t)\gamma_2(t) \right] dt, \tag{4.11}$$

where $\Gamma = \partial\Omega$, ν is the outward unit normal to Γ, and $\big(\gamma_1(\cdot), \gamma_2(\cdot)\big)$ is a parametrization of Γ. Here it assumed for simplicity that Γ is connected. If, on the other hand, $k \neq 0$, then

$$\tilde{I}_k = \frac{1}{2\pi} \int_\Omega e^{ik\cdot x}\, dx = \frac{1}{2\pi|k|^2} \int_\Omega -\Delta e^{ik\cdot x}\, dx$$

$$= -\frac{1}{2\pi|k|^2} \int_\Gamma \nu \cdot \nabla e^{ik\cdot x}\, d\sigma_\Gamma = -\frac{i}{2\pi|k|^2} \int_\Gamma [k \cdot \nu] e^{ik\cdot x}\, d\sigma_\Gamma$$

$$= \frac{i}{2\pi|k|^2} \int_0^{2\pi} \left[k_2 \dot{\gamma}_1(t) - k_1 \dot{\gamma}_2(t) \right] e^{ik\cdot\gamma(t)}\, dt. \tag{4.12}$$

Thus, given a representation of Ω via its boundary Γ, either as a list of points (from which the relevant geometric quantities can be computed) or via an analytic expression (often available even in pratice), the computation reduces to that of a periodic one dimensional integral which can be performed to high accuracy as already noted earlier. The advantage of this approach is that the integrand lives on B, or on G^m, and only a simple discrete representation Γ^n of Γ is needed in order to perform the calculation. Notice that the grids G^m and Γ^n do not need to have any relation whatsoever to one another. In fact, when u is smooth, m can be kept small while n will need to be chosen large in order to get a good approximation of the highly oscillatory (in general) line integral. The advantage clearly lies in the line integral being one dimensional.

4.2. **Boundary Value Problems.** Let again Ω be a smooth domain inside the box B and consider the classical boundary value problems

$$\begin{cases} -\Delta u = f & \text{in } \Omega, \\ u = g & \text{on } \Gamma, \end{cases} \tag{4.13}$$

and

$$\begin{cases} u - \Delta u = f & \text{in } \Omega, \\ \partial_\nu u = g & \text{on } \Gamma, \end{cases} \tag{4.14}$$

where it can be assumed that the data are given as $f : B \to \mathbb{R}$ and $g : \Gamma \to \mathbb{R}$. Using

$$G(x,y) = G(x-y) = \frac{1}{2\pi} \log(|x-y|) \text{ for } x, y \in \mathbb{R}^2,$$

and the classical Green's identity

$$\int_\Omega (u\Delta G - G\Delta u)\, dx = \int_\Gamma (u\partial_\nu G - G\partial_\nu u)\, d\sigma_\Gamma, \tag{4.15}$$

solution representations can be obtained from

$$u(x) = \int_\Omega G(x,y)f(y)\, dy - \int_\Gamma G(x,y)\partial_\nu u(y)\, d\sigma_\Gamma(y) + \int g(y)\partial_\nu G(x,y)\, d\sigma_\Gamma(y),$$

$$u(x) = \int_\Omega G(x,y)f(y)\, dy + \int_\Gamma u(y)\partial_\nu G(x,y)\, d\sigma_\Gamma(y) - \int G(x,y)g(y)\, d\sigma_\Gamma(y),$$

once the boundary functions u and $\partial_\nu u$ are recovered, depending on whether one considers the Neumann or Dirichlet problem, respectively. While the single and double layer potentials terms

$$\mathcal{S}(u)(x) = \int_\Gamma G(x,y)\partial_\nu u(y)\, d\sigma_\Gamma(y),\ x \in \mathbb{R}^2 \setminus \Gamma, \tag{4.16}$$

$$\mathcal{D}(u)(x) = \int_\Gamma u(y)\partial_\nu G(x,y)\, d\sigma_\Gamma(y),\ x \in \mathbb{R}^2 \setminus \Gamma. \tag{4.17}$$

are important to understand and will appear later for their mapping properties, the construction of solutions, both analytical and numerical, presented here will proceed slightly differently. The following facts [2] will be useful

$$S(u)(x) = \lim_{\Gamma \not\ni \tilde{x} \to x} \mathcal{S}(u)(\tilde{x}) = \int_\Gamma G(x,y)\partial_\nu u(y)\, d\sigma_\Gamma(y),\ x \in \Gamma, \tag{4.18}$$

$$\partial_{\nu\pm} S(u)(x) = \lim_{\Omega^\pm \ni \tilde{x} \to x} \partial_\nu(\tilde{x})S(u)(\tilde{x}) = \mp\frac{1}{2}u(x) + N(u)(x),\ x \in \Gamma, \tag{4.19}$$

where $\Omega^+ = \Omega$ and $\Omega^- = \mathbb{R}^2 \setminus \overline{\Omega}$, respectively, and the normal to Γ is extended continuously in a neighborhood of Γ, and

$$N(u)(x) = \int_\Gamma u(y)\partial_{\nu(x)}G(x,y)\, d\sigma_\Gamma(y),\ x \in \Gamma.$$

The starting point consists in observing that the function $G(\cdot,y)$ is a harmonic function in Ω for any $y \in B \setminus \Omega$ and for any fundamental solution G. For the Dirichlet problem therefore take

$$G_\pi^D(x,y) = G_\pi\big((x-y) \bmod 2\pi - \pi\big),$$

to be the Green's function for the periodicity box B characterized by its symbol

$$\hat{G}_\pi^D(k) = \begin{cases} 0, & k = 0, \\ \frac{1}{|k|^2}, & 0 \neq k \in \mathbb{Z}^2, \end{cases}$$

and, for the Neumann problem, G_π^N with symbol

$$\hat{G}_\pi^N(k) = \frac{1}{1 + |k|^2}, \; k \in \mathbb{Z}^2.$$

If f is a mean zero function, i.e. if $\hat{f}_0 = 0$, then $G_\pi^D * f = \int_B G_\pi^D(\cdot, y) f(y) \, dy$ satisfies

$$-\Delta G_\pi^D * f = f \text{ in } \Omega,$$

as desired. One also has that

$$G_\pi^D * \left(-\Delta u\right) = u - P_0(u),$$

where $P_0 = (\cdot | e_0) e_0$ is the orthogonal projection onto the subspace consisting of constant functions. Similarly for the Neumann problem where

$$(1 - \Delta) G_\pi^N * f = f \text{ and } G_\pi^N * \left(u - \Delta u\right) = u.$$

A solution to the boundary value problems can therefore be sought in the form

$$u(x) = G_\pi^b * f(x) + \int_\Gamma G_\pi^b(x, y) h(y) \, d\sigma_\Gamma(y), \; x \in \Omega, \; b = D, N,$$

where the second term is a "harmonic" function in Ω and can be thought of as a superposition along the boundary of functions in the kernel of Δ_Ω or $1 - \Delta_\Omega$, respectively, which generate the desired boundary behavior for the solution. The function h can indeed be determined by the requirement that $u = g$ or $\partial_\nu u = g$ on the boundary Γ, respectively, that is by insisting that

$$g(x) = \langle \delta_x, u \rangle = \langle \delta_x, G_\pi^D * f \rangle + \langle \delta_x, G_\pi^D * (h \delta_\Gamma) \rangle, \; x \in \Gamma,$$

and that

$$g(x) = \langle -\nu(x) \cdot \nabla \delta_x, u \rangle = -\langle \partial_{\nu(x)} \delta_x, G_\pi^N * f \rangle - \langle \partial_{\nu_x} G_\pi^N * (h \delta_\Gamma) \rangle, \; x \in \Gamma,$$

where

$$H * (h \delta_\Gamma) = \int_\Gamma H(x, y) h(y) \, d\sigma_\Gamma(y),$$

for $H = G_\pi^D, \partial_{\nu_x} G_\pi^N$. The above is justified by the fact that

$$\partial_\nu u(x) = \langle \delta_x, \partial_\nu u \rangle = \langle \delta_x, \sum_{j=1}^2 \nu_j \partial_j u \rangle = \sum_{j=1}^2 \langle \nu_j \delta_x, \partial_j u \rangle$$

$$= \sum_{j=1}^2 \langle \nu_j(x) \delta_x, \partial_j u \rangle = -\langle \nu(x) \cdot \nabla \delta_x, u \rangle$$

$$= -\langle \partial_{\nu(x)} \delta_x, u \rangle, \; x \in \Gamma.$$

This yields an equation

$$M_b(h) = \check{g} = \begin{cases} g - \langle \delta., G_\pi^D * f \rangle, & b = D, \\ g + \langle \nu. \cdot \nabla \delta., G_\pi^N * f \rangle, & b = N, \end{cases}$$

for an operator M_b on Γ given by

$$M_b(h) = \int_\Gamma m_b(x, y) h(y) \, d\sigma_\Gamma(y), \; h : \Gamma \to \mathbb{R}, \tag{4.20}$$

with kernel function defined by

$$m_b(x, y) = \begin{cases} m_D(x, y) = \langle \delta_x, (-\Delta_\pi)^{-1} P_\psi \delta_y \rangle, & b = D, \\ m_N(x, y) = \langle \partial_{\nu(x)} \delta_x, (1 - \Delta_\pi)^{-1} P_\psi \delta_y \rangle, & b = N, \end{cases} \text{ for } x, y \in \Gamma, \tag{4.21}$$

for the Dirichlet and Neumann problem, respectively. Here the more transparent notation $(-\Delta_\pi)^{-1}$ and $(1 - \Delta_\pi)^{-1}$ are used for the operation of convolution with G_π^D and G_π^N, respectively. $P_\psi u$ denotes the projection onto mean zero functions/distributions given by

$$P_\psi u = u - \hat{u}_0 \psi = u - \tilde{u}_0 \psi, \tag{4.22}$$

for a nonnegative function $\psi \in \mathcal{D}_\pi$ satisfying

$$\text{supp}(\psi) \subset \Omega^\complement \text{ and } \hat{\psi}_0 = 1. \tag{4.23}$$

Remark 4.1. *Using the suggestive notation*

$$d\sigma_\Gamma(y) = |\langle dy, \frac{\partial}{\partial t}\rangle| dt,$$

for $\langle dy, \frac{\partial}{\partial t}\rangle = \dot{\gamma}(t)$ when $y = \gamma(t)$ to evoke the validity of

$$\int_\Gamma v(y)\, d\sigma_\Gamma(y) = \int_0^{2\pi} v\big(\gamma(t)\big)|\dot{\gamma}(t)|\, dt,$$

for any parametrization γ of Γ and for any smooth integrand $v : \Gamma \to \mathbb{R}$, allows for the factor $|\langle dy, \frac{\partial}{\partial t}\rangle|$ to be assimilated into the unknown function h to yield $|\langle dy, \frac{\partial}{\partial t}\rangle|h$ as the new unknown. This is particularly convenient when working at the discrete level, where one is only eventually interested in the function

$$x \mapsto \int_\Gamma G_\pi^b(x,y) h(y)\, d\sigma_\Gamma(y) = \int_0^{2\pi} G_\pi^b(x,y) h(y)|\langle dy, \frac{\partial}{\partial t}\rangle|\, dt,\ \Omega \to \mathbb{R}$$

and the determination of h or $|\langle dy, \frac{\partial}{\partial t}\rangle|h$ are equivalent.

The kernels m_D and m_N in (4.21) have the form of those considered in the previous section and are of exactly the same type as in the earlier one dimensional toy boundary value problem. Just as in that case, δ_y can be replaced by $\delta_{\tilde{y}}$ for

$$\tilde{y} = y + \delta\nu(y),\ y \in \Gamma,$$

where $\delta > 0$ can be chosen such that a tubular neighborhood

$$T_\Gamma^\delta = \{x \in B \,|\, d(x,\Gamma) < 2\delta\}$$

of Γ can be found with well-defined coordinates $(y,s) \in \Gamma \times (-2\delta, 2\delta)$ satisfying

$$x = y + s\nu(y) \text{ for } y = Y(x) \text{ and } s = d(x,\Gamma).$$

This corresponds to replacing Γ by $\widetilde{\Gamma} = \{\tilde{y} \,|\, y \in \Gamma\}$ in the evaluation of the kernel (but not in that of the boundary integral). Notice that latter distinction is immaterial at the discrete level where the boundary measure is assimilated in the unknown function h as described above. An even better choice is obtained by replacing δ_y by

$$\varphi_{\tilde{y}} \in \mathcal{D}_0 \text{ with } \text{supp}(\varphi_{\tilde{y}}) \subset \Omega^\complement \text{ and } \text{supp}(\varphi_{\tilde{y}}) \cap \text{supp}(\psi) = \emptyset. \tag{4.24}$$

The kernel modification is shown pictorially in Figure 1.

The upshot is that the operator M^b with singular kernel is replaced by the operator $\widetilde{M}^b$ with smooth kernel given by

$$\begin{cases} \widetilde{m}_D(x,y) = \langle \delta_x, (-\Delta_\pi)^{-1} P_\psi \varphi_{\tilde{y}} \rangle, & b = D, \\ \widetilde{m}_N(x,y) = \langle \partial_{\nu(x)}\delta_x, (1 - \Delta_\pi)^{-1} P_\psi \varphi_{\tilde{y}} \rangle, & b = N, \end{cases} \text{ for } x, y \in \Gamma.$$

By choosing $\varphi_{\tilde{y}}$ localized enough (read close to a Dirac delta function) it follows that

$$M^b - \widetilde{M}^b \simeq 0,$$

The figure shows:

$$\text{supp}(\varphi_{\tilde{y}})$$

$$\nu_\Gamma(y)$$

$$\Gamma$$

$$\tilde{y}$$

$$y$$

$$G_\pi(x,y) = \langle \delta_x, (-\triangle_\pi)^{-1} P_\psi \delta_y \rangle$$

$$\wr|$$

$$\widetilde{G}_\pi(x,y) = \langle \delta_x, (-\triangle_\pi)^{-1} P_\psi \varphi_{\tilde{y}} \rangle$$

$$\Omega$$

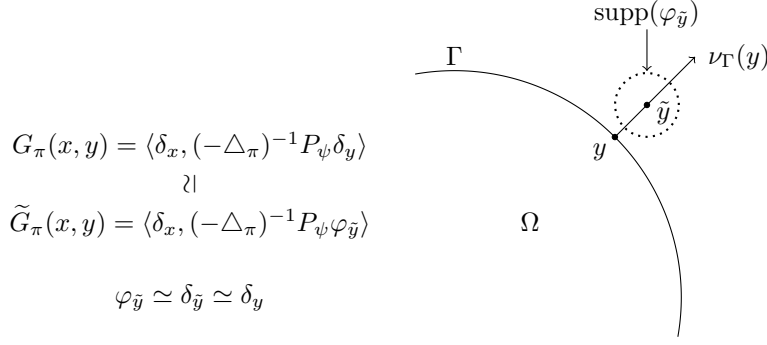$$\varphi_{\tilde{y}} \simeq \delta_{\tilde{y}} \simeq \delta_y$$

FIGURE 1. A pictorial illustration of the proposed kernel construction.

in the strong operator sense. Notice that the projection procedure (4.23) ensures that the support of $P_\psi \varphi_{\tilde{y}}$ lies completely outside of Ω and does thus still generate functions in the kernel of Δ_Ω.

Remark 4.2. *The operator M^b can be shown to be smoothing of one degree of differentiability in the Dirichlet case, and of none in the Neumann case. For a proof based on symbol analysis see e.g. [2].*

Remark 4.3. *While it is often convenient to work with an explicit fundamental solution for $-\Delta$ and use it in order to derive the necessary boundary kernels (to be used in a numerical implementation of boundary integral type), the approach described above does not rely on the explicit knowledge of a Green's function. Indeed at the discrete level, the kernel functions, $G_\pi^D = (-\Delta_\pi)^{-1}$ and $G_\pi^N = (1 - \Delta_\pi)^{-1}$ in the examples, can be replaced by $(A_D^m)^{-1}$ and $(A_N^m)^{-1}$ for any discretizations A_b^m to the grid G^m of a differential operator A_b obtained by spectral or finite difference methods for $b = D, N$. In the above example A^m would be a standard spectral or finite difference approximations of the periodic Δ and $1-\Delta$ operators on the box B. This opens the door to applying the method to nonconstant coefficient operators and to constant coefficient operators for which no explicit Green's function or symbol is available.*

Next an illustrative analytical result is proved in the Dirichlet case which will play an important role in obtaining invertibility results for the numerical schemes derived later.

Lemma 4.4. *The operator M^D defined in (4.20) with kernel m_D given by (4.21) is invertible.*

Proof. First notice that G_π^D is a fundamental solution on the space of mean zero distributions. It follows either from Poisson's summation formula or from the theory of pseudodifferential operators [2] that G_π^D is smooth away from the diagonal $[x = y]$ and that

$$G_\pi^D(x,y) \simeq \frac{1}{2\pi} \log\big(|x - y|\big) = G(x,y), \ x \simeq y \in B,$$

i.e., it has the same singular behavior of the full space fundamental solution G. It indeed differs from it by a smooth kernel only. Now one has that

$$m_D(x,y) = \sum_{k \in \mathbb{Z}^2} e^{ik \cdot x} \frac{1}{|k|^2} \big(e^{-ik \cdot y} - \hat{\psi}_k\big) = \sum_{0 \neq k \in \mathbb{Z}^2} e^{ik \cdot x} \frac{1}{|k|^2} \big(e^{-ik \cdot y} - \hat{\psi}_k\big)$$

and thus that

$$m_D(x,y) = G_\pi^D(x,y) - \sum_{0 \neq k \in \mathbb{Z}^2} e^{ik \cdot x} \frac{\hat{\psi}_k}{|k|^2} = G_\pi^D(x,y) - \eta(x),$$

where η is a smooth function. Consequently one sees that

$$\widetilde{S}(h) = \int_\Gamma G_\pi^D(\cdot, y) h(y) \, d\sigma_\Gamma(y) - \eta(x) \int_\Gamma h(y) \, d\sigma_\Gamma(y).$$

This means that $\widetilde{S}$ enjoys the same classical jump relations as S given by

$$S(h) = \int_\Gamma G(\cdot, y) h(y) \, d\sigma_\Gamma(y),$$

i.e. it holds

$$\begin{cases} \gamma_\gamma^+ \widetilde{S}(h) = \gamma_\gamma^- \widetilde{S}(h) = \gamma_\Gamma \widetilde{S}(h), \\ \partial_{\nu_\Gamma^+} \widetilde{S}(h) - \partial_{\nu_\Gamma^-} \widetilde{S}(h) = h, \end{cases} \tag{4.25}$$

where the superscripts $\pm$ indicate limits taken from within and from without Ω, respectively, just as in (4.18). It also follows (see e.g. [2]) that M^D is Fredholm and that it continuously maps $\mathrm{H}^s(\Gamma)$ to $\mathrm{H}^{s+1}(\Gamma)$ for any $s \in \mathbb{R}$. It is therefore enough to show that M^D is injective "on smooth functions", i.e. that

$$\gamma_\Gamma \widetilde{S}(h) = \gamma_\Gamma \int_\Gamma m_D(\cdot, y) h(y) \, d\sigma_\Gamma(y) = 0 \Longrightarrow h \equiv 0,$$

for smooth $h : \Gamma \to \mathbb{R}$. Since $\widetilde{S}(h)$ is defined for all $x \in B$ and is harmonic in $B \setminus \Gamma$, unique solvability of the Dirichlet problem in Ω yields that $\widetilde{S}(h)\big|_\Omega \equiv 0$. By construction it holds that

$$\int_B \widetilde{S}(h) \, dx = 0,$$

so that Poincaré's inequality

$$\int_{B \setminus \Omega} \widetilde{S}(h)^2 \, dx = \int_B \widetilde{S}(h)^2 \, dx \le c \int_B \left| \nabla \widetilde{S}(h) \right|^2 dx = c \int_{B \setminus \Omega} \left| \nabla \widetilde{S}(h)^2 \right| dx,$$

entails that, if $\widetilde{S}(h)\big|_{B \setminus \Omega}$ is constant, then it has to vanish identically. Since

$$0 = -\int_{B \setminus \Omega} \widetilde{S}(h) \Delta \widetilde{S}(h) \, dx = \int_{B \setminus \Omega} \left| \nabla \widetilde{S}(h) \right|^2 dx - \int_\Gamma \underbrace{\widetilde{S}(h)}_{=0} \partial_\nu \widetilde{S}(h) \, d\sigma_\Gamma,$$

it therefore follows that $\widetilde{S}(h)\big|_{B \setminus \Omega} \equiv 0$. Finally this shows that

$$\partial_{\nu_\Gamma^-} \widetilde{S}(h)\big|_{B \setminus \Omega} = -h = 0,$$

thus establishing the claim. $\square$

Proposition 4.5. *The modified operator $\widetilde{M}^D$ is injective provided $\tilde{y} \simeq y$ and $\varphi_{\tilde{y}} \simeq \delta_{\tilde{y}}$ for $y \in \Gamma$.*

Proof. The operator $\widetilde{M}^D$ has smooth kernel and is therefore compact. Given any smooth $h \not\equiv 0$, it follows from the previous lemma that $\gamma_\Gamma \widetilde{S}(h) \not\equiv 0$. Now it holds that

$$\langle \delta_x, (-\Delta_\pi)^{-1} P_\psi \varphi_{\tilde{y}} \rangle \to \langle \delta_x, (-\Delta_\pi)^{-1} P_\psi \delta_{\tilde{y}} \rangle \text{ as } \varphi_{\tilde{y}} \to \delta_{\tilde{y}},$$

pointwise everywhere in $x, y \in \Gamma$ (in fact, uniformly). On the other hand, one also has that

$$\delta_{\tilde{y}} \to \delta_y \text{ as } \tilde{y} \to y,$$

uniformly in $y \in \Gamma$ in the sense of distributions (or in the sense of measures) so that

$$\langle \delta_x, (-\Delta_\pi)^{-1} \delta_{\tilde{y}} \rangle \to \langle \delta_x, (-\Delta_\pi)^{-1} \delta_y \rangle \text{ as } \tilde{y} \to \tilde{y},$$

pointwise for $x \neq y$, i.e., almost everywhere. Since the limiting kernel is integrable in view of its logarithmic behavior in the singularity and provides a bound for the approximating kernels, Lebesque's theorem yields that

$$\langle \delta_x, (-\Delta_\pi)^{-1} \delta_{\tilde{y}} \rangle \to m_D(x, y) \text{ in } \mathrm{L}^1(\Gamma, d\sigma_\Gamma(y)),$$

uniformly in $x \in \Gamma$, and, in fact, uniformly in $|x - y| \geq \varepsilon$ for any $\varepsilon > 0$. Consequently

$$\widetilde{M}^D(h) \to M^D(h) \text{ as } \tilde{\Gamma} \to \Gamma,$$

uniformly in $\big[\|h\|_2 = 1 \big]$ due to the mild (in particular square integrable) singularity of m_D on the diagonal. This then entails that

$$\ker(\widetilde{M}^D) = \{0\},$$

for $\tilde{\Gamma}$ close enough to Γ. □

This useful property will remain valid after discretization, which is just an additional approximation, even if, as will be demostrated in the numerical examples, the modified and the original boundary are not that close to each other.

Remark 4.6. *The result shows that the functions $w_{\tilde{y}} : \Omega \to \mathbb{R}$ given by*

$$w_{\tilde{y}}(x) = \int_B G_\pi^D(x, z) P_\psi \varphi_{\tilde{y}}(z) \, dz \text{ for } y \in \Gamma$$

are "linearly independent" elements of $\ker(\Delta_\Omega)$ if $\tilde{\Gamma} \simeq \Gamma$ and $\varphi_{\tilde{y}} \simeq \delta_{\tilde{y}}$. This is intuitively clear for $\tilde{\Gamma} = \Gamma$ and $\varphi_{\tilde{y}} \simeq \delta_y$ since, then, w_y are functions with singularities at different locations $x = y$, yielding a "diagonally dominant" kernel (or matrix, at the discrete level).

Remark 4.7. *When dealing with the Neumann problem in the classical way, the fact that the normal derivative of S is not continuous across Γ as clearly indicated by (4.18), does require care in obtaining the correct numerical formulation. By using the kernel generation procedure described in this paper, however, the problem is completely avoided, since the relevant kernel $\widetilde{m}_N$ is smooth thanks to the replacement of δ_y by $\varphi_{\tilde{y}}$ in its construction.*

Remark 4.8. *Notice that the proposed kernel construction effectively replaces a pseudo-differential operator of type -1 or type 0 for $b = D$ or $b = N$, respectively, with an infinitely smoothing operator. Incidentally, an operator of type k is a bounded linear operator which maps, in the above context, $\mathrm{L}^2(\Gamma)$ to $\mathrm{H}^{-k}(\Gamma)$. This has important consequences. One is that the approximating operator is compact with unbounded inverse (more so that the approximated operator), i.e. it does not enjoy the same "functional" mapping properties. At the numerical level this will be reflected in a significant increase in the condition number of the discretized operator. It will, however, be possible to use natural "rougher" discretizations of the same operator as preconditioners, thus completely curing the conditioning issues, while maintaining the highly desirable fast converging numerical discretizations to the approximate smooth kernel and, consequently, accuracy.*

5. Numerical Implementation and experiments

The periodc box $B = [-\pi, \pi]^2$ is discretized by a uniform grid G^m of 2^{2m} points by discretizing each direction by

$$z_j^m = -\pi + 2\pi \frac{j}{2^m}, \ j = 0, \ldots, 2^m - 1,$$

where $z = x_1, x_2$. The boundary value problems will be posed on the unit circle centered at the origin, i.e. $\Omega = \mathbb{B}(0, 1)$ and the padding function ψ of (4.23) is defined by

$$\psi(x_1, x_2) = e^{-200 \sin^2[\frac{1}{2}(x_1 - \pi)] \sin^2[\frac{1}{2}(x_2 - \pi)]}.$$

While it is not analytically compactly supported away from Ω, it numerically vanishes outside a neighborhood of the boundary of the periodicity box B as show in the contourplot below. The boundary of the domain Ω is discretized by n equidistant points

$$y_j = \big(\cos(\theta_j), \sin(\theta_j)\big),\ j = 0, ..., n-1,$$

where $\theta_j = 2\pi \frac{j}{n}$, yielding the set Γ^n. Wherever required, the analytical knowledge of the boundary Γ of Ω will be used to obtain numerical quantities such as, e.g., normal and tangent vectors. In some applications these might need to be replaced by their numerical counterparts.
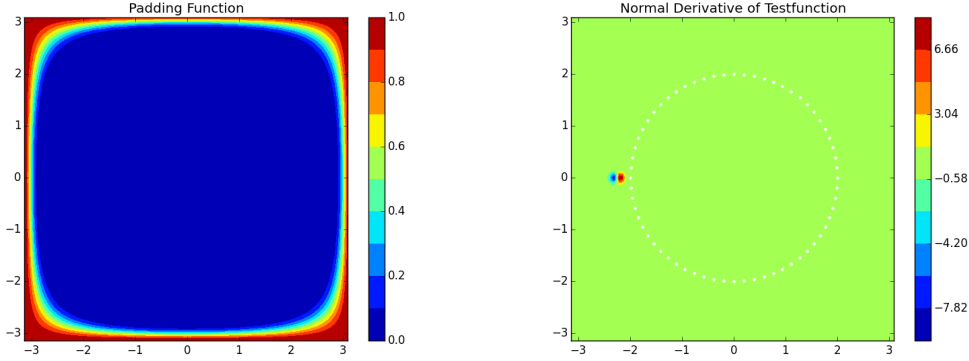
At the chosen discretization level m, the discrete Laplace operator $-\triangle^m$ on the periodicity box is represented spectrally via discrete Fast Fourier transform $\mathcal{F}_m$ via

$$\mathcal{F}_m^{-1}\operatorname{diag}\big[(|k|^2)_{k\in\mathbb{Z}_{2^m}^2}\big]\mathcal{F}_m.$$

The projection P_ψ of (4.22) is discretized by

$$P_\psi^m(u^m) = u^m - \frac{\mathcal{F}_m(u^m)(0,0)}{\mathcal{F}_m(\psi^m)(0,0)}\psi^m,$$

where u^m is a grid vector, i.e. a function defined on the grid G^m and ψ^m is the evaluation of ψ on it. The testfunctions $\varphi_{\tilde{y}}$ supported about the point $\tilde{y} \in B \setminus \Omega$ used in the set up of the kernel are chosen of two different types: symmetric and non-symmetric. The former are defined through

$$\varphi_{\tilde{y}}(z) = e^{-\alpha\sin^2[\frac{1}{2}(z_1-\tilde{y}_1)]\sin^2[\frac{1}{2}(z_2-\tilde{y}_2)]},\ z \in B$$

and are discretized by evaluation on the grid G^m and setting $\alpha = 2^{m+2}$ in order to make the testfunction "sharper" compatibly with the resolution power of the grid. For reasons to be explained later, non-symmetric and "sharper" testfunctions are useful. Given a point $y \in \Gamma = \mathbb{S}^1$, let $\tau = \tau(y)$ and $\nu = \nu(y)$ denote the corresponding unit tangent and normal vector, respectively. Then consider

$$\partial_\nu\varphi_{\tilde{y}}, \tag{5.26}$$

where the reader is reminded that

$$\tilde{y} = y + \delta\nu(y),\ y \in \Gamma.$$

This type of testfunction, depicted in the contourplot above, has the added adavantage of automatically having vanishing average, and plays an important role in deriving efficient numerical discretizations (see Subsection 5.2.2).

TABLE 1. Relative error for the Fourier quadrature rule at different discretization levels.

m	n	$e^{m,n}$	m	n	$e^{m,n}$
32	128	3.78e-03	128	128	4.30e-08
	256	3.78e-03		256	4.33e-08
	512	3.78e-03		512	4.33e-08
64	128	1.80e-04	192	128	3.07e-07
	256	1.80e-04		256	2.58e-07
	512	1.80e-04		512	2.58e-07
96	128	8.73e-06	256	128	1.81e-08
	256	8.73e-06		256	4.05e-08
	512	8.73e-06		512	4.05e-08

5.1. **Bulk Integrals.** As a first example consider the domain integral as described in Section 4.1. Letting $\Omega = \mathbb{B}(0,2)$ and computing the Fourier coefficients $\tilde{I}_k$ of the distribution $I = \chi_\Omega$ just as explained in (4.11)-(4.12) by using the trapezoidal rule for the angular parametrization of $\mathbb{S}^2_2$, one obtains a quadrature rule for integration over Ω. Table 1 summarizes the results obtained when applying the quadrature to the function

$$u = \cos(\frac{\pi}{4}r^2), \ r > 0.$$

It appears that the number of discretization points n has less of an impact on the accuracy than the bulk discretization level m as can be expected since the integrand is radially symmetric.

5.2. **Dirichlet Problem.** Consider now the Dirichlet Problem on $\mathbb{B}(0,1)$ and take the right hand side to be $f \equiv 1$ defined on whole square B. In a first step, a function a grid vector v^m is determined satisfying

$$-\triangle^m v^m \equiv 1.$$

This can be done simply by taking

$$v^m = \mathcal{F}_m^{-1} \operatorname{diag}\big[(g_\pi^m(k))_{k \in \mathbb{Z}^2_{2m}}\big] \mathcal{F}_m\big(P_\psi^m(1^m)\big) =: G_\pi^m(1^m),$$

where 1^m is the constant grid function with value 1 and

$$g_\pi^m(k) = \begin{cases} 0, & \text{if } k = (0,0), \\ |k|^{-2}, & \text{if } k \in \mathbb{Z}^2_m \setminus \{(0,0)\}. \end{cases}$$

Next the boundary weight vector w^n is determined such that

$$\big\langle \delta_{y_j}^m, v^m + \sum_{k=1}^n w_k^n G_\pi^m(\varphi_{\tilde{y}_k}^m) \big\rangle_{q^m} = 0 \text{ for } k = 0, \ldots, n-1.$$

This leads to a system of equations for the entries of w^n characterized by the matrix M with entries

$$M_{jk} = \big\langle \delta_{y_j}^m, G_\pi^m(\varphi_{\tilde{y}_k}^m) \big\rangle_{q^m}, \ j, k = 1, \ldots, n,$$

TABLE 2. Numerical Results for the Dirichlet Problem, $\delta = 0.4$

m	n	$e_\infty^{m,n}$	$e_2^{m,n}$	cond(M)	m	n	$e_\infty^{m,n}$	$e_2^{m,n}$	cond(M)
6	64	2.12e-05	3.18e-05	2.6e+03	8	128	2.17e-11	1.71e-11	1.7e+06
	80	1.33e-05	2.90e-05	1.7e+04		144	1.61e-11	4.83e-12	8.3e+06
	96	1.10e-05	2.75e-05	1.1e+05		160	3.01e-11	7.16e-12	3.9e+07
	112	6.11e-05	1.42e-04	1.1e+08	9	64	1.30e-06	1.10e-06	2.5e+03
7	64	1.03e-06	1.01e-06	2.5e+03		80	5.44e-08	4.74e-08	1.3e+04
	80	1.94e-07	1.62e-07	1.3e+04		96	2.43e-09	2.14e-09	6.9e+04
	96	2.07e-07	9.92e-08	7.0e+04		112	1.14e-10	9.89e-11	3.5e+05
8	64	1.26e-06	1.10e-06	2.5e+03		128	5.48e-12	4.68e-12	1.7e+06
	80	5.43e-08	4.74e-08	1.3e+04		144	2.75e-13	2.24e-13	8.3e+06
	96	2.32e-09	2.13e-09	6.9e+04		160	2.38e-14	6.39e-15	3.9e+07
	112	1.17e-10	1.01e-10	3.5e+05		176	2.44e-14	6.30e-15	1.8e+08

following the blueprint laid out in the previous section. It can be viewed as being close to the spectral discretization

$$k^m(x,y) = \langle \delta_x^m, (-\triangle^m)^{-1} P_\psi^m(\delta_{\tilde{y}}^m) \rangle_{q^m}, \ x, y \in \Gamma^n \subset \mathbb{S}^1.$$

of the smooth kernel

$$k(x,y) = \langle \delta_x, (-\triangle)^{-1} P_\psi(\delta_{\tilde{y}}) \rangle, \ x, y \in \mathbb{S}^1.$$

As mentioned earlier this discretization k^m is actually independent of the grid G^m and can be evaluated anywhere in $B \times B$, in particular on $\Gamma^n \times \Gamma^n$. It follows from Proposition 4.5 that M is invertible for appropriate choices of $\tilde{y}$ for $y \in \Gamma^n$ and of testfunctions $\varphi_{\tilde{y}}$. Once the grid vector w^m is found, a numerical solution of the Dirichlet problem is given by

$$r_\Omega^m u^{m,n} = r_\Omega^m \left(v^m + \sum_{k=1}^n w_k^n G_\pi^m(\varphi_{\tilde{y}_k}^m) \right),$$

where r_Ω^m denotes the restriction (of functions defined on B or of vectors defined on the grid G^m) to $G^m \cap \Omega$. The numerical results presented in Table 2 provide information about the relative l_2 and l_∞ errors $e_2^{m,n}$ and $e_\infty^{m,n}$ computed as follows

$$e_p^{m,n} = \frac{\|r_\Omega^m u^{m,n} - r_\Omega^m u\|_{l_p}}{\|r_\Omega^m u\|_{l_p}} \text{ for } p = 2, \infty,$$

This is done for various combined discretization levels (m,n), various distances of $\tilde{y}$ from $y \in \Gamma^n$, and types of testfunctions in Tables 2–4. Recorded is also the condition number of the obtained matrix M. The results with fixed distance $\delta = 0.4$ are summarized in Table 2. It appears clearly that accuracy tends to grow for a given grid parameter m with increasing number of boundary discretization points n. This happens until the boundary discretization becomes too fine compared to the given, fixed discretization of the periodicity box. Notice that, if the parameter n is kept fixed, the accuracy improves also as a function of the discretization size m. Similarly gains stop accruing when the box discretization becomes too fine compared to the fixed boundary resolution. As the operator approximated by M is of negative order 1, the condition number of M is expected

TABLE 3. Dependence on $\delta = \mathrm{dist}(\Gamma, \widetilde{\Gamma})$ for $m = 8$

n	δ	$e_\infty^{m,n}$	$e_2^{m,n}$	$\mathrm{cond}(M)$	n	δ	$e_\infty^{m,n}$	$e_2^{m,n}$	$\mathrm{cond}(M)$
64	0.15	9.06e-04	8.69e-04	9.6e+01	80	0.5	2.59e-09	2.09e-09	6.2e+04
	0.2	2.28e-04	2.18e-04	1.9e+02		0.6	1.54e-10	1.05e-10	2.7e+05
	0.3	1.58e-05	1.45e-05	7.1e+02		0.7	3.84e-11	1.12e-11	1.2e+06
	0.4	1.26e-06	1.10e-06	2.5e+03		0.8	2.95e-11	1.06e-11	4.9e+06
	0.5	1.15e-07	9.33e-08	8.3e+03	144	0.15	6.10e-06	1.02e-05	3.9e+03
	0.6	1.20e-08	8.90e-09	2.7e+04		0.2	4.13e-08	3.81e-08	1.9e+04
	0.7	1.42e-09	9.41e-10	8.6e+04		0.3	1.01e-10	1.02e-10	4.3e+05
	0.8	1.80e-10	9.65e-11	2.6e+05		0.4	1.61e-11	4.83e-12	8.3e+06
	0.9	6.59e-11	2.09e-11	7.9e+05	192	0.15	2.85e-08	1.40e-08	2.9e+04
80	0.15	2.42e-04	2.06e-04	2.1e+02		0.2	3.95e-10	3.63e-10	2.5e+05
	0.2	4.24e-05	3.77e-05	5.1e+02		0.3	1.04e-13	7.99e-14	1.6e+07
	0.3	1.40e-06	1.24e-06	2.7e+03		0.35	1.94e-14	2.96e-15	1.3e+08
	0.4	5.43e-08	4.74e-08	1.3e+04					

to grow linearly in the discretization size. Indeed increasing n enlarges the condition number. This effect is, however, compounded by the matrix M becoming less and less diagonally dominant as the boundary discretization points become denser while the support of the testfunctions remains unchanged for fixed discretization level m. Notice that, for fixed n, the condition number of M remains virtually unchanged as m changes. The "optimal" value (for the specific choice of testfunction type and support size) was chosen based on the results found in Table 3 where the arbitrary but still representative choice of $m = 8$ is made and a variety of discretization levels n are shown. The distance is steadily increased until it no longer leads to an improvement in the approximation quality. It can be seen that the accuracy improves with distance and that optimal distance decreases as the box discretization gets finer, thus allowing for a stronger resolution power and, consequently, a better approximation of the testfunctions. There appears to be a trade-off between condition number of M and accuracy of the outcome, where the best accuracy is obtained at the cost of a high condition number. In perfect agreement with the theoretical analysis, the condition number of M is the least when using Dirac delta functions located along the discrete boundary Γ^n in the numerical representation of the kernel. This is clearly evident in the data shown in Table 4 for two choices of discretization level, $m = 7, 8$. Again the low condition number comes at the price of a reduced accuracy (if the comparison is carried out at the same discretization level m).

5.2.1. *Preconditioning.* Given the dramatic increase in condition number resulting from the use of the proposed smoother kernels, it is natural to ask whether it can be mitigated by some preconditioning procedure. Denote by M_φ and M_δ the matrix obtained discretizing the smooth kernel and the singular kernel, respectively, i.e.

$$M_\varphi = \left\langle \delta_{y_j}^m, G_\pi^m\left(\varphi_{\tilde{y}_k}^m\right) \right\rangle_{q^m}, \; j, k = 1, \ldots, n,$$

TABLE 4. Kernel based on Dirac delta functions supported along Γ.

m	n	$\mathrm{cond}(M)$	$e_\infty^{m,n}$	$e_2^{m,n}$	m	n	$\mathrm{cond}(M)$	$e_\infty^{m,n}$	$e_2^{m,n}$
7	64	10.9	5.49e-02	4.93e-02	8	96	14.34	4.43e-02	4.67e-02
	80	15.05	4.06e-02	2.72e-02		112	18.06	3.46e-02	3.46e-02
	96	21.16	2.59e-02	1.57e-02		124	21.49	2.74e-02	2.51e-02
	112	26.01	1.25e-02	7.50e-03		144	25.58	2.32e-02	1.81e-02
	128	31.88	7.06e-03	2.31e-03		160	29.83	2.17e-02	1.36e-02
	144	38.78	1.05e-02	7.72e-03		176	36.52	1.58e-02	1.03e-02
8	64	8.42	8.27e-02	9.57e-02		192	42.51	1.20e-02	7.80e-03
	80	11.26	6.09e-02	6.61e-02		208	47.22	1.13e-02	5.66e-03

and
$$M_\delta = \left\langle \delta_{y_j}^m, G_\pi^m\left(\delta_{y_k}^m\right)\right\rangle_{q^m}, \; j,k = 1,\ldots,n.$$

It seems natural to use the better conditioned but "rough" approximation M_δ as a preconditioner for the highly accurate but badly conditioned M_φ. In Table 5 the condition numbers of M_φ, M_δ, and $C = M_\delta^{-1} M_\varphi$ are shown for a few discretization levels. They clearly point to an enormous benefit of preconditing. The plots in Figure 2 gives a more visual characterization of the effect of preconditioning on the diagonal dominance of the corresponding matrix.
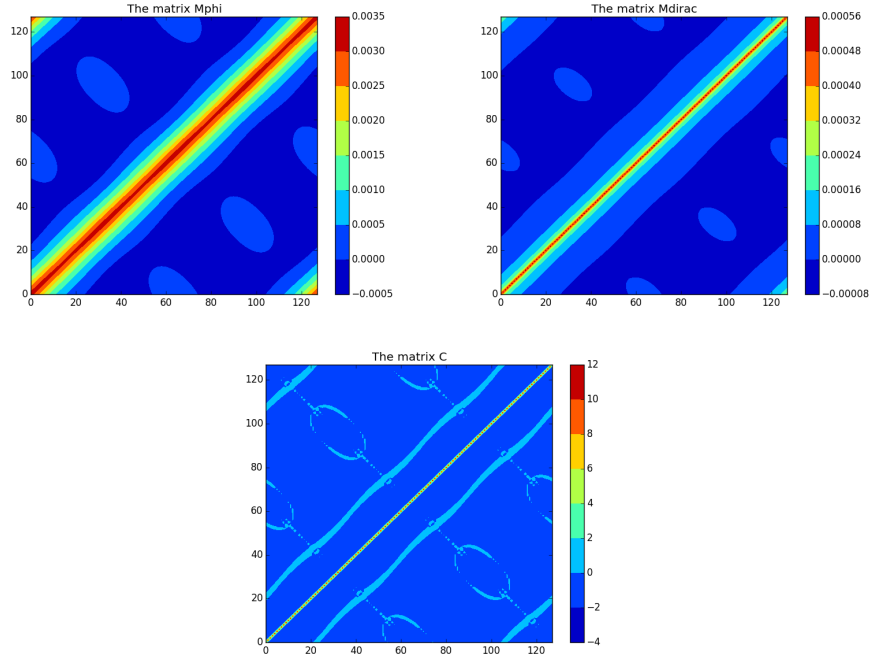

FIGURE 2. Contour plot of M_φ, M_δ, and $C = M_\delta^{-1} M_\varphi$ for $m = 8$, $n = 128$, and $\delta = 0.4$.

TABLE 5. Preconditioning effect of M_δ^{-1} on M_φ when $\delta = 0.4$.

(m, n)	$\mathrm{cond}(M_\varphi)$	$\mathrm{cond}(M_\delta)$	$\mathrm{cond}(M_\delta^{-1} M_\varphi)$
$(7, 64)$	2.51e+03	1.09e+01	5.24e+00
$(8, 128)$	1.72e+06	2.15e+01	1.01e+01
$(9, 256)$	4.02e+11	4.27e+01	1.96e+01

It can therefore be concluded that smoother kernels lead to higher order resolutions and more accurate numerical results at the cost of at the apparent increased condition number. Latter can, however, be completely avoided by a simple and natural preconditioning procedure.

5.2.2. *Effective Numerical Implementation.* The necessity to project a datum onto the subspace of mean zero functions in the above procedure effectively destroys the translation invariance of the constant coefficients equation on the periodic box. This makes it necessary to compute a box solution for each entry of the matrix M. While it was chosen to illustrate the ideas using test-functions $\varphi_{\tilde{y}}$ approximating Dirac distributions δ_y in order to harvest the benefits of the theoretical analysis ensuring injectivity (and thus invertibility) of M, it is clear that other choices are possible, such as normal derivatives of testfunctions. These are particularly suited since they are mean zero functions supported in a small neighborhood of their "center-point". As such they do not require to be projected onto the mean free subspace. It is therefore enough to compute

$$(-\Delta_\pi)^{-1}\partial_{\nu(y)}\varphi_{\tilde{y}} = \sum_{j=1}^{2}\nu_j(y)(-\Delta_\pi)^{-1}\partial_j\varphi_{\tilde{y}}$$

for one point $y \in \Gamma$ only since

$$(-\Delta_\pi)^{-1}\partial_j\varphi_{\tilde{y}+v} = (-\Delta_\pi)^{-1}\tau_v(\partial_j\varphi_{\tilde{y}}) = \tau_v(-\Delta_\pi)^{-1}\partial_j\varphi_{\tilde{y}}, \ j = 1, 2,$$

where $\tau_v u = u(\cdot - v)$ is the translation of a periodic function u. This also gives insight into the "circulant" structure of the matrix M.

It is also possible to replace the test-function centers $\{\tilde{y} : y \in \Gamma\}$ by nearby or closest (box) grid points in G^m so that the translations required to obtain the kernel from the knowledge of, say, $(-\Delta_\pi)^{-1}\partial_{\nu(y_1)}\varphi_{\tilde{y}_1}$, can be implemented efficiently (i.e. in physical space).

Remark 5.1. *Notice that, if Δ is replaced by a more general elliptic non-constant coefficient differential operator, the kernel construction given above is still viable and would deliver a purely numerical boundary integral method which which does not rely on the explicit analytical knowledge of a fundamental solution for the differential operator. It even allows replacing the "discrete" fundamental solution by a smooth kernel which can more accurately be captured numerically. Remarkably this can be done at effectively not cost due to the availability of the natural preconditioning procedure described above.*

Remark 5.2. *The proposed construction of smooth kernels also suggests that iterative parallelized methods can be used in the computation of the entries of the matrix M with a small number of iterations in the case of a non-constant coefficient differential operator $\mathcal{A}$, at least when the coefficients vary smoothly. This is due to the fact that the building blocks $\mathcal{A}_\pi^{-1}\varphi_{\tilde{y}}$ will be locally close to each other thus providing excellent initial guesses for an iterative solver.*

5.2.3. *Kernel Functions.* Ultimately the accuracy of the method rests on its ability to faithfully compute linearly independent functions in the kernel of the Laplacian Δ_Ω^D on the domain Ω. These are known explicitly for $\Omega = \mathbb{B}(0,2)$ and given by

$$\psi_k(r,\theta) = (\frac{r}{2})^k e^{ik\theta}, \ r \in [0,2], \ \theta \in [0,2\pi), \ k \in \mathbb{N},$$

in polar coordinates. Using the method described above, it is possible to compute a numerical approximation of these functions defined on G^m. Tables 6 and 7 give the relative errors observed for the first 33 kernel functions at two distinct discretization levels.

TABLE 6. Resolution of the first 33 kernel functions for $m = 7$, $n = 80$, and $\delta = 0.4$.

	ℓ_∞-err	ℓ_2-err		ℓ_∞-err	ℓ_2-err		ℓ_∞-err	ℓ_2-err
ψ_1	1.84e-07	8.11e-08	ψ_{12}	1.08e-05	9.60e-06	ψ_{23}	1.43e-03	9.88e-04
ψ_2	1.72e-07	9.16e-08	ψ_{13}	2.14e-05	1.39e-05	ψ_{24}	2.05e-03	1.57e-03
ψ_3	3.45e-07	2.08e-07	ψ_{14}	3.65e-05	2.28e-05	ψ_{25}	3.68e-03	2.36e-03
ψ_4	5.99e-07	3.60e-07	ψ_{15}	5.80e-05	3.13e-05	ψ_{26}	4.40e-03	3.51e-03
ψ_5	1.21e-06	5.73e-07	ψ_{16}	7.81e-05	5.81e-05	ψ_{27}	6.87e-03	5.60e-03
ψ_6	1.23e-06	8.65e-07	ψ_{17}	1.10e-04	7.28e-05	ψ_{28}	1.17e-02	9.09e-03
ψ_7	2.53e-06	1.32e-06	ψ_{18}	1.60e-04	1.04e-04	ψ_{29}	1.97e-02	1.32e-02
ψ_8	4.29e-06	2.66e-06	ψ_{19}	2.99e-04	1.72e-04	ψ_{30}	2.76e-02	2.14e-02
ψ_9	5.50e-06	2.92e-06	ψ_{20}	3.10e-04	2.63e-04	ψ_{31}	3.84e-02	3.08e-02
ψ_{10}	5.59e-06	4.38e-06	ψ_{21}	6.44e-04	4.12e-04	ψ_{32}	4.99e-02	4.63e-02
ψ_{11}	1.26e-05	6.32e-06	ψ_{22}	1.07e-03	6.35e-04	ψ_{33}	9.99e-02	7.05e-02

5.3. **Neumann Problem.** Next, using the same notations and discretization procedure, the Neumann problem

$$\begin{cases} u - \triangle u = f & \text{in } \Omega = \mathbb{B}(0,2), \\ \partial_\nu u = 0 & \text{on } \Gamma = 2\mathbb{S}^1, \end{cases} \tag{5.27}$$

for $f(x) = \cos(\frac{\pi}{2}r)\big(1 + \frac{\pi^2}{4}\big) + \frac{\pi}{2}\sin(\frac{\pi}{2}r)/r$, $r = \sqrt{x_1^2 + x_2^2}$ and $x \in B$. This problem has the exact solution u given by $u(x) = \cos\big(\frac{\pi}{2}r(x)\big)$, $x \in \Omega$. In order to show that the method is robust in the sense that it does not depend on the exact choices of its ingredients, a different cutoff function is used in order to modify the right-hand-side f to make it into a doubly periodic function which fits the periodic framework. More specifically, take

$$\psi(x) = \frac{1}{2}\big\{1 + \tanh\big(-\frac{5}{2}[r - (\pi - 0.2)^2]\big)\big\},$$

which essentially vanishes close to the the boundary of B and takes the value 1 on Ω. Replace then f by $\tilde{f} = f\psi$ to obtain a periodic function which coincides with f on Ω. In numerical experiments,

TABLE 7. Resolution of the first 33 kernel functions for $m = 9$, $n = 256$, and $\delta = 0.4$.

	ℓ_∞-err	ℓ_2-err		ℓ_∞-err	ℓ_2-err		ℓ_∞-err	ℓ_2-err
ψ_1	1.24e-13	1.09e-14	ψ_{12}	1.57e-13	5.68e-14	ψ_{23}	6.23e-13	2.63e-13
ψ_2	9.17e-14	1.10e-14	ψ_{13}	1.90e-13	5.43e-14	ψ_{24}	7.15e-13	4.11e-13
ψ_3	1.29e-13	1.63e-14	ψ_{14}	1.34e-13	5.18e-14	ψ_{25}	9.98e-13	4.19e-13
ψ_4	1.23e-13	1.90e-14	ψ_{15}	2.03e-13	6.65e-14	ψ_{26}	1.25e-12	5.38e-13
ψ_5	1.22e-13	2.00e-14	ψ_{16}	2.73e-13	8.48e-14	ψ_{27}	1.52e-12	6.23e-13
ψ_6	1.04e-13	2.24e-14	ψ_{17}	2.65e-13	9.30e-14	ψ_{28}	1.48e-12	7.26e-13
ψ_7	1.31e-13	2.58e-14	ψ_{18}	3.68e-13	1.15e-13	ψ_{29}	1.99e-12	9.46e-13
ψ_8	1.14e-13	2.87e-14	ψ_{19}	3.73e-13	1.16e-13	ψ_{30}	1.80e-12	1.04e-12
ψ_9	1.23e-13	3.03e-14	ψ_{20}	4.03e-13	2.01e-13	ψ_{31}	2.77e-12	1.27e-12
ψ_{10}	1.10e-13	3.18e-14	ψ_{21}	5.31e-13	1.82e-13	ψ_{32}	3.38e-12	1.80e-12
ψ_{11}	1.74e-13	3.64e-14	ψ_{22}	4.84e-13	2.58e-13	ψ_{33}	3.50e-12	1.83e-12

this is clearly performed on the grid, i.e. by replacing f^m by $\tilde{f}^m = \psi^m f^m$. The solution procedure is parallel to that employed for the Dirichlet problem. First the function

$$v^m = (1^m - \triangle^m)^{-1}\tilde{f}^m = \mathcal{F}_m^{-1} \operatorname{diag}\left(\left(\frac{1}{1 + |k|^2}\right)_{k \in \mathbb{Z}_m^2}\right)\mathcal{F}_m(\tilde{f}^m)$$

is computed. Then the kernel matrix M is obtain as

$$M_{jk} = \left\langle -\left(\partial_{\nu(y_j)}\delta_{y_j}\right)^m, (1^m - \triangle^m)^{-1}\varphi_{\tilde{y}_k}^m\right\rangle_{q^m}, \; j, k = 1, \ldots, m,$$

where

$$-\left(\partial_{\nu(y_j)}\delta_{y_j}\right)^m = -\nu_1(y_j)(\delta'_{y_j^1})^m \otimes \delta_{y_j^2}^m - \nu_2(y_j)\delta_{y_j^1}^m \otimes (\delta'_{y_j^2})^m$$

is used as a discretization of the normal derivative operator at the point $(y_j^1, y_j^2) = y_j \in \Gamma^n$. Finally the weight vector w^n is determined by solving

$$\left\langle -\left(\partial_{\nu(y_j)}\delta_{y_j}\right)^m, v^m + \sum_{k=1}^{n} w_k^n (1^m - \triangle^m)^{-1}\varphi_{\tilde{y}_k}^m\right\rangle_{q^m} = z + Mw^n = 0,$$

where $z_j = \left\langle -\left(\partial_{\nu(y_j)}\delta_{y_j}\right)^m, v^m\right\rangle_{q^m}$ for $j = 1, \ldots, n$. Results of similar numerical experiments to those performed for the Dirichlet problem are summarized in Table 8.

Remark 5.3. *Notice that in all numerical experiments, radially symmetric functions were used. One reason is that radial symmetry is not readily compatible with periodicity in that it cannot be represented with very few periodic modes. Another is that explicit formulæ are available.*

Remark 5.4. *While it might appear that in the construction of the matrix kernel M, one needs to solve n problems in the discretized periodicity box, this is not always the case. As for the Dirichlet problem, the operator $1 - \triangle$ is translation invariant. It follows that it is enough to solve one such problem, e.g. for $k = 1$ since all other solutions would be a translate of the solution for $k = 1$. This is true because the datum $\varphi_{\tilde{y}_k}$ is a translate of $\varphi_{\tilde{y}_1}$. To make sure that the translation be compatible with the grid G^m, the theoretical location $\tilde{y} = y + \delta\nu_\Gamma(y)$ would have to be replaced by the closest grid point in G^m (for instance).*

TABLE 8. Numerical experiments for the Neumann problem (5.27).

m	n	δ	cond(M)	$e_\infty^{m,n}$	$e_2^{m,n}$	m	n	δ	cond(M)	$e_\infty^{m,n}$	$e_2^{m,n}$
5	32	0.3	3.31e+00	4.84e-03	2.97e-03	7	64	0.3	2.82e+01	2.59e-04	2.55e-04
		0.4	6.04e+00	8.67e-03	4.94e-03			0.4	9.83e+01	2.12e-05	2.02e-05
		0.5	9.61e+00	3.99e-03	3.86e-03			0.5	3.27e+02	6.24e-06	4.44e-06
	48	0.3	9.98e+00	1.31e-02	1.20e-02	8	64	0.3	2.84e+01	2.65e-04	2.56e-04
		0.4	2.85e+01	1.22e-02	9.84e-03			0.4	9.82e+01	1.91e-05	1.84e-05
		0.5	1.79e+02	3.37e-03	2.35e-03			0.5	3.26e+02	1.53e-06	1.47e-06
6	32	0.3	3.14e+00	2.18e-02	2.08e-02		128	0.3	2.46e+03	3.41e-08	3.34e-08
		0.4	5.45e+00	5.58e-03	5.57e-03			0.4	3.33e+04	4.41e-10	1.75e-10
		0.5	9.38e+00	2.39e-03	2.19e-03			0.5	4.08e+05	5.96e-10	3.87e-10
	48	0.3	9.36e+00	1.70e-03	1.36e-03	9	128	0.3	2.46e+03	3.43e-08	3.35e-08
		0.4	2.33e+01	5.51e-04	3.24e-04			0.4	3.33e+04	2.65e-10	1.93e-10
		0.5	5.35e+01	2.94e-04	1.42e-04			0.5	4.08e+05	1.05e-10	3.95e-11
	64	0.3	2.90e+01	1.38e-04	5.22e-05		256	0.3	1.88e+07	1.76e-10	7.73e-11
		0.4	9.89e+01	6.46e-04	5.20e-04			0.4	3.88e+09	1.76e-10	7.72e-11
		0.5	3.48e+02	3.98e-04	3.53e-04			0.5	6.47e+11	1.76e-10	7.72e-11

6. Conclusions

An effectively meshless approach to boundary value problem in general geometry domains is proposed based on the use of uniform discretizations of an encopassing computational box. Exploiting a pseudodifferential operator framework, relevant kernels can be replaced by smoother kernels which allow for more accurate numerical resolution. No explicit knowledge of the kernels is required beyond their analytical structure which is used in an essential way in order to construct their numerical counterparts. While the smooth kernels, which correspond to infinitely smoothing compact operators, and their associated discretization matrices are badly ill-conditioned, they can very effectively be preconditioned by use of their "rougher" counterparts with singular kernels in an arguably natural way at minimal additional cost. The methodology proposed is very general and can be employed in three space dimensions as well as to more general linear and nonlinear boundary value problems. The fact that no remeshing is required makes this method particularly appealing for free and moving boundary. These extensions will be the topic of forthcoming papers.

References

[1] P. Guidotti. Numerical Approximation of Generalized Functions: Aliasing, the Gibbs Phenomenon and a Numerical Uncertainty Principle. In *Functional Analysis and Evolution Equations*, Volume Dedicated to the Memory of Günther Lumer. Birkhäuser, 2007.
[2] M. E. Taylor. *Partial Differential Equations II. Qualitative Studies of Linear Equations.* Springer-Verlag, New York, 1996.

University of California, Irvine, Department of Mathematics, 340 Rowland Hall, Irvine, CA 92697-3875, USA

E-mail address: gpatrick@math.uci.edu